jove Journal of Visualized Experiments www.jove.com

Video Article

Localization and Relative Quantification of Carbon Nanotubes in Cells with Multispectral Imaging Flow Cytometry

Iris Marangon*[1], Nicole Boggetto*[2], Cécilia Ménard-Moyon[3], Nathalie Luciani[1], Claire Wilhelm[1], Alberto Bianco[3], Florence Gazeau[1]

[1]Laboratoire Matière et Systèmes Complexes (MSC), CNRS/Université Paris Diderot

[2]ImagoSeine BioImaging Core Facility, Institut Jacques Monod, CNRS/Université Paris Diderot

[3]Laboratoire d'Immunopathologie et Chimie Thérapeutique, CNRS/Institut de Biologie Moléculaire et Cellulaire

*These authors contributed equally

Correspondence to: Florence Gazeau at florence.gazeau@univ-paris-diderot.fr

URL: http://www.jove.com/video/50566
DOI: doi:10.3791/50566

Keywords: Bioengineering, Issue 82, bioengineering, imaging flow cytometry, Carbon Nanotubes, bio-nano-interactions, cellular uptake, cell trafficking

Date Published: 12/12/2013

Citation: Marangon, I., Boggetto, N., Ménard-Moyon, C., Luciani, N., Wilhelm, C., Bianco, A., Gazeau, F. Localization and Relative Quantification of Carbon Nanotubes in Cells with Multispectral Imaging Flow Cytometry. *J. Vis. Exp.* (82), e50566, doi:10.3791/50566 (2013).

Abstract

Carbon-based nanomaterials, like carbon nanotubes (CNTs), belong to this type of nanoparticles which are very difficult to discriminate from carbon-rich cell structures and *de facto* there is still no quantitative method to assess their distribution at cell and tissue levels. What we propose here is an innovative method allowing the detection and quantification of CNTs in cells using a multispectral imaging flow cytometer (ImageStream, Amnis). This newly developed device integrates both a high-throughput of cells and high resolution imaging, providing thus images for each cell directly in flow and therefore statistically relevant image analysis. Each cell image is acquired on bright-field (BF), dark-field (DF), and fluorescent channels, giving access respectively to the level and the distribution of light absorption, light scattered and fluorescence for each cell. The analysis consists then in a pixel-by-pixel comparison of each image, of the 7,000-10,000 cells acquired for each condition of the experiment. Localization and quantification of CNTs is made possible thanks to some particular intrinsic properties of CNTs: strong light absorbance and scattering; indeed CNTs appear as strongly absorbed dark spots on BF and bright spots on DF with a precise colocalization.

This methodology could have a considerable impact on studies about interactions between nanomaterials and cells given that this protocol is applicable for a large range of nanomaterials, insofar as they are capable of absorbing (and/or scattering) strongly enough the light.

Video Link

The video component of this article can be found at http://www.jove.com/video/50566/

Introduction

During the last decades, the place of nanoparticles has gained in importance in a wide range of applications. In particular, carbon nanotubes (CNTs) are more and more explored as nanotools for diverse diagnostic and therapeutic applications; thanks to their particular electrical, thermal, and spectroscopic properties, CNTs can act as delivery vehicles for varied drugs or contrast agents, or can also be involved in tissue engineering[1].

However, concerns about the potential toxicity of such nanomaterials are still under debate, mainly because the fate of CNTs in the organism remains very controversial. There is indeed a lack of appropriate methods to detect and quantify them in live cells and tissues: for example, techniques such as Raman spectroscopy, photoacoustic, and near-infrared photoluminescence imaging have been suggested, but each method shows limitations depending on the type of nanotubes and/or their environment[2-8].

Here, the method proposed could be applicable for the detection and quantification of nanoparticles in cells. This was made possible by the use of ImageStream, a device combining both flow cytometry and high resolution imaging. It couples the advantages of acquiring a large among of cells (up to 5000 events/sec) - and benefits of statistical data and high resolution images of each cell at the same time (0.5 µm spatial resolution). Generally, images are collected using a CCD camera and are a two dimensional grey scale representation of the cell. The light is quantified for each pixel in the image and identifies both the intensity and the location of either fluorescence or components with a subcellular size (in BF for example), allowing thus a powerful ability to discriminate cells based on their appearance[9,10].

The aim was here to design a nanometrology method which would enable a quantitative assessment of the distribution and behavior of CNTs in cells. In particular, this method was developed to study cellular uptake, processing and exocytosis of CNTs by cells. We evidenced first the complex cellular trafficking of CNTs and secondly the transfer of these nanomaterials between cells: cell-internalized CNTs escape their host cells when stressed, spread abroad in the extracellular space and are reinternalized by naïve cells, whether they are homotypic or heterotypic[11]

.

Previous study showed that different mechanisms of cell uptake, either active or passive ones, could occur depending on CNT functionalization and aggregation state[12]. Here the multi-walled CNTs were functionalized through 1,3-dipolar cycloaddition and amidation and then derivatized with a fluorescent probe, fluoresce in isothiocyanate (FITC). On transmission electron microscopy, they appear to be internalized by cells either individually with cytosolic localization or as bundles, mostly found in endosomal and lysosomal compartments[11]. On ImageStream, the clustered CNTs appear with a high correlation as dark spots on BF and bright spots on DF, allowing a clear distinction between CNT-labeled cells and control cells. On the other hand, the distribution of the fluorescent signal emitted by the fluorescent marker functionalized with CNTs was not as well colocalized: indeed, likely due to a quenching phenomenon, the green fluorescent spots do not necessarily match the spots on BF and DF. This indicates that, firstly, a fluorescent probe is not mandatory for the detection of CNTs with the ImageStream, and secondly - *a fortiori* - that it is not fully representative for both quantification and localization of CNTs.

Beyond giving a statistical relative *quantification* of nanoparticles, this method also provides information concerning the *localization* of CNTs in cells, meaning that it discriminates, for instance, CNTs on the interior of the cell versus those which are bound to the plasma membrane. The ability to localize CNTs on cell images clearly overcomes the limitation of conventional flow cytometry analysis[13]. The procedure was developed here via the creation of masks fitting with specific regions of the cell and selecting also the dark spots corresponding to loaded CNTs.

Generally speaking, this method could be applied for a large range of experiments involving the need of visualization, or quantification, in cells on condition that the nanoparticles used are able to strongly absorb (and/or scatter) the light.

Protocol

1. Preparation of Water Dispersible Carbon Nanotubes (CNTs)

1. Disperse first CNTs in cell culture water, before sonicating them for 20 min in a bath-water sonicator at 20 °C. If CNTs are functionalized with a fluorescent probe, protect them as much as possible from light throughout the experiment.

2. Labeling Cells with CNTs

1. Grow human umbilical vein endothelial cells (HUVEC) (for example) on 25 cm² plates in DMEM medium, containing 10% fetal bovine serum and 1% penicillin streptomycin.
2. Prepare solutions of CNTs at concentration of 0, 10, 20, and 50 µg/ml in complete medium and incubate cells with at 37 °C for 20 hr or at 4 °C for 20 hr (2ml of CNT suspension for a 25 cm² plate).

3. Cell Fixation

1. Remove incubation medium afterwards; rinse cells with PBS, trypsinize, and resuspend cells in complete DMEM medium. Centrifuge for 5 min at 1,200 rpm.
2. Replace the medium first by paraformaldehyde 4% for 1 hr at 4 °C, then by PBS to preserve them. If needed, cells can be stored at this stage of the process at 4 °C for several days until the cytometry analysis.
3. Each sample has to contain about 10^6 cells concentrated in 50 µl of PBS. Suspend them correctly to avoid aggregates during the analysis and filter them through a 50 µm mesh stainer.
   ***Note**: Each step has to be performed very gently to preserve cells.*

4. ImageStream Acquisition

Use the multispectral imaging flow cytometer ImageStream to acquire images of cells.
Some points have to be respected:

1. Select an adapted magnification (here a 40X objective is used).
2. If fluorochromes are used:
   - prepare a control sample without fluorochrome.
   - prepare cells with a single-color positive control for each fluorochrome used in addition to your samples.
3. Use the laser 488 nm to excite the FITC and the channel 02 to collect the fluorescence emission (band-pass 480-560 nm). In addition, use also the channels 01 and 06 for the bright field (BF) and dark field(DF) respectively.

5. Post Processing - IDEAS Analysis Software (Version 4.0)

1. Among all the events acquired, the analysis has to be first restricted to the population of single cells: use a biparametric dot plot representing 'aspect ratio' (*i.e.* width/height) versus 'cell area' (parameters applied on cells on BF) (**Figure 1**). Single cells included in the region of interest with a standard area and aspect ratio close to 1 are then discriminated from multicellular events (large area and small aspect ratio) and debris (extremely small area).
2. To select cells in the focused plane, use a biparametric dot plot adapted for highly contrasted CNTs-labeled cells: plot the 'contrast' versus the 'RMS gradient' (which measures the sharpness quality of an image) on the BF image - it allows the exclusion of unfocused cells showing both a low rms gradient and a low contrast in their BF images (**Figure 1**).

3. 1. Determine the parameter which provides the best statistical separation between labeled and nonlabeled cells by using the "find the best feature". In our study, the mean pixel object feature is the parameter which is the most suitable (**Figure 2**).
   2. Trace an histogram using this parameter versus the normalized frequency to compare the quantity of uptaken-CNTs for tested concentrations (**Figure 3**).
   3. Trace the biparametric graph 'mean pixel object on BF' (*Notation: Mean Pixel_Object (M01,Ch01,Tight)_Ch01*) versus 'intensity on DF'(*Intensity_MC_Ch06*), in order to study the correlation between these two parameters (**Figure 4**).

4. The quantification is also assessed by means of masks:
   1. As CNTs appears as strongly absorbing dark spots on BF, create first a threshold mask that fit them precisely by selecting a restricted range of pixels with a low intensity comprised between 0-533 in this study *(Mask 1, notation: Intensity(M01, BF, 0-533))* (**Figure 5**). The choice of the threshold intensity is made on labeled cells in comparison to the control cells.
   2. Conversely create also a mask fitting with the pixels of high intensity (150-4095 in this case) of the DF *(Mask 2, notation: Intensity (M06, DF, 150-4095))* (**Figure 6**).
   3. Plot a graph using the area of the mask (either 1 or 2; (*notation: Area_Intensity(M01, BF, 0-533)*for mask 1): it will provide a relative quantification of the internalization of CNTs at different concentrations (**Figure 7**).
   4. Check the degree of correlation between these two masks (thanks to the biparametric plot 'area of Mask 1' versus 'area of Mask 2') (**Figure 7**).

5. Create other masks to localize CNTs in cells:
   1. A mask fitting the interior of the cell: *Erode(M01, 7)* - corresponding to the mask of the entire cell (M01) (**Figure 8**), which is further eroded of 7 pixels (**Figure 9**).
   2. A mask fitting the membrane only using the Boolean equation: *M01 and not Erode(M01,7)* - mask of the entire cell (M01) subtracted from the interior (Erode(M01,7)) (**Figure 10**).
   3. To consider the dark pixels on the membrane (corresponding to CNTs), create then the mask: *Intensity(M01 and not Erode(M01, 7), BF, 0-533)* (**Figure 11**).
   4. Visualize the different masks applied on a collection of cells to check their relevance (**Figure 12**) for labeled and unlabeled cells.
   5. Apply the feature area on the mask selecting the black pixels on the membrane 'Area_*Intensity(M01 and not Erode(M01, 7), BF, 0-533)'* so called black area. It will allow the quantification of the CNTs on the membrane.
      To discriminate finally CNTs that have been internalized from those adsorbed only on the membrane, plot the black area on the membrane versus the black area on the entire cell (*i.e.* 'Area_ *Intensity(M01 and not Erode(M01, 7), BF, 0-533'* versus *'Area_ Intensity(M01, BF, 0-533)').*
      Note: The same type of procedure is applied with the FITC-fluorescent signal: compare the increase of the intensity of FITC fluorescence *versus* the decrease of the mean pixel signal on the BF, or the colocalization between dark spots on BF and FITC fluorescence intensity. In our case, this type of analysis is not relevant because fluorescence signal does not correctly match with dark spots on BF on one hand and with bright field on DF on the other hand, showing that intrinsic properties of CNTs (light absorbance and scattering) are more appropriate than the signal related to the fluorescence probe.

6. Once all plots are created on one experimental condition create a "statistical report template", save template as .ast file and batch all data files.

Representative Results

An overview of the principle of the ImageStream device is given in **Figure 1**. It produces multiple high resolution images of each cell in flow, including bright-field (BF), dark-field (DF or side-scattered light), and fluorescence channel(s), as exemplified in **Figure 2** with three different cells labeled with CNTs. The overlays of these channels are also shown, at first sight illustrating the correlation.

Given that all the post-processing analysis is based on cell imaging, the selection of focused cells is crucial for the study (**Figure 3**). Actually, the presence of CNTs induces changes on both the contrast and the gradient compared to nonlabeled cells: focused cells, having internalized an important quantity of CNTs, tend to have a low rms gradient (which is usually the unique parameter used for the discrimination of focused *versus* unfocused cells) but also an important contrast, explaining why a biparametric plot is essential. On **Figure 3** is shown the discrimination between unfocused (yellow area) *versus* focused cells (blue area).

Cell-internalized CNTs are clearly distinguishable - particularly on BF appearing as strongly absorbing dark spots (see the effect of diverse labeling concentration, **Figure 4**). Moreover, the mean pixel signal on BF was analyzed, giving a relative quantification of the uptake: graphs on **Figure 5** show its significant increase with the CNT-labeling concentration (results for about 7,000 cells per experimental condition).

Second, quantification of CNTs is also possible through the use of masks, applied either on a restricted range of dark pixels of the BF or on the pixel of high intensity of the DF (see examples on **Figure 6**), corresponding to the spots resulting from the presence of CNTs. Thus, plotting the area of these masks allows highlighting as well as the increase of the uptake (exemplified on **Figure 7** with the area of the mask on BF, selecting pixels ranging from 0-533).

In addition, the correlation between spots on BF and DF can be evaluated by plotting the DF intensity versus the BF mean pixel signal (as in **Figure 8**) (mask-independent analysis) or the area of the mask on BF (Mask 1) versus the area on DF (Mask 2).

Regarding the procedure created for the localization of CNTs inside the cells, **Figure 9A** displays the different masks that were created. Note that the robustness of the localization masks (based on erosion of default cell mask) must be checked visually on a collection of labeled and unlabeled cells. The same masks are used for all samples.

Plotting the total area of black spots on the cell membrane *versus* that on the entire cell provides a score of internalization for cells which have been incubated for 20 hr at 37 °C in comparison to 2 hr incubation at 4 °C (see **Figure 9B**); it indicates that CNTs are mostly located on the membrane at 4 °C, whereas at 37 °C CNTs are internalized in more than 90% of cells.

Finally concerning the fluorescence, this parameter was not used as indicator for the quantification of CNTs due to a too low correlation between fluorescent spots and spots on BF (and DF). Indeed, the correlation between the FITC intensity and the bright field mean pixel indicates a Pearson correlation coefficient of -0.2. On **Figure 10**, two cases are illustrated, in which the fluorescence signal matches properly or not with the bright field black spot.

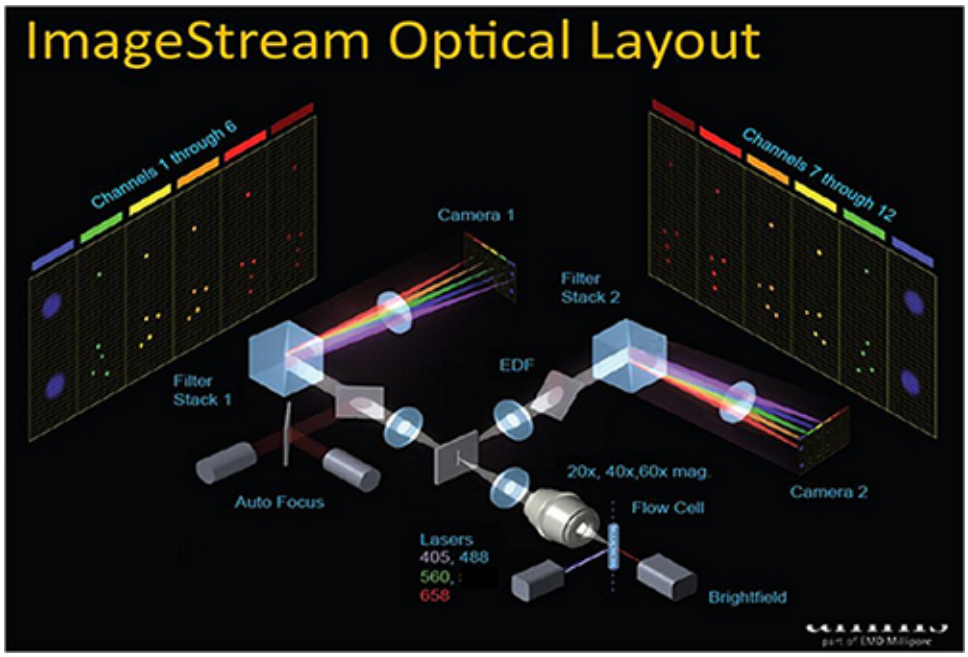

Figure 1. Overview of the ImageStream- general operating. The multispectral imaging system acquires up to 12 images/cell in three different modes: brightfield, darkfield, and fluorescence. The setup consists in 5 excitation lasers, including 405, 488, 560, and 658 nm. Light is collected from the cells flowing in the cuvette with different objective lens (in this study, the 40X objective lens was used) and relayed to the spectral decomposition element, which consists in a set of longpass filters in an angular array. The CCD camera collecting cell images is operated using a technique called time-delay-integration in order to avoid image streaking. Extended depth of field (EDF) is an option.

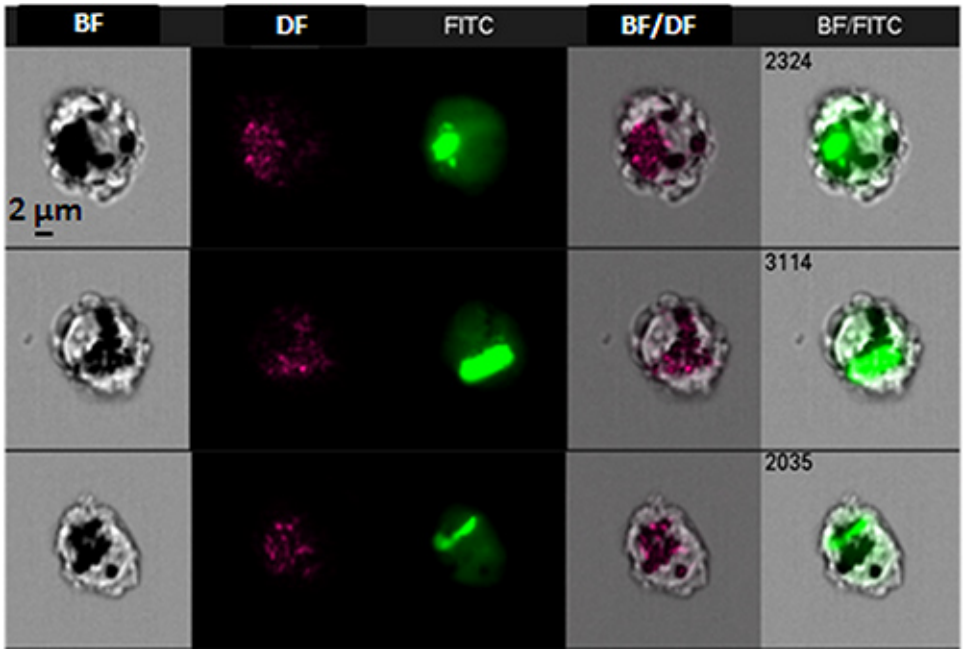

Figure 2. Image gallery of cells labeled with carbon nanotubes (50 µg/mL) captured by ImageStream through diverse channels (Bright Field (BF), Dark field (DF), fluorescence (FITC), and their overlays). CNTs confined within intracellular lysosomes appear as large black spots on bright field images. Conversely they create bright spots on the dark field and on the fluorescence images.

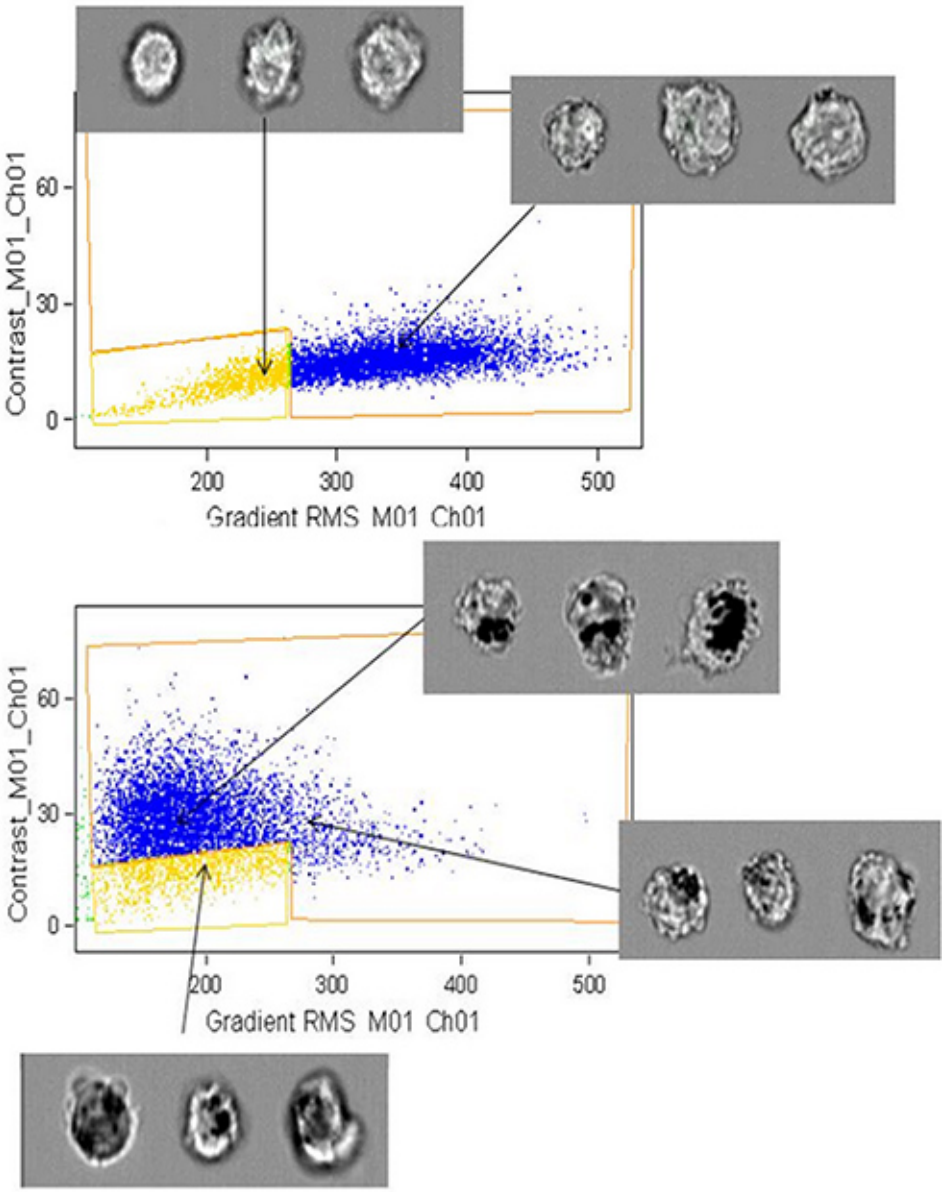

Figure 3. Selection of cells in focus. Bivariate dot plot representing root mean square (rms) gradient versus contrast on BF images allows the exclusion of unfocused cells. Here the yellow area represents unfocused cells, whereas focused cells are represented in blue. The unfocused cells are characterized by both low contrast and low gradient rms on the bright field image. In addition to rms gradient, the contrast feature is require to discriminate focused cells after their labeling with CNTs.

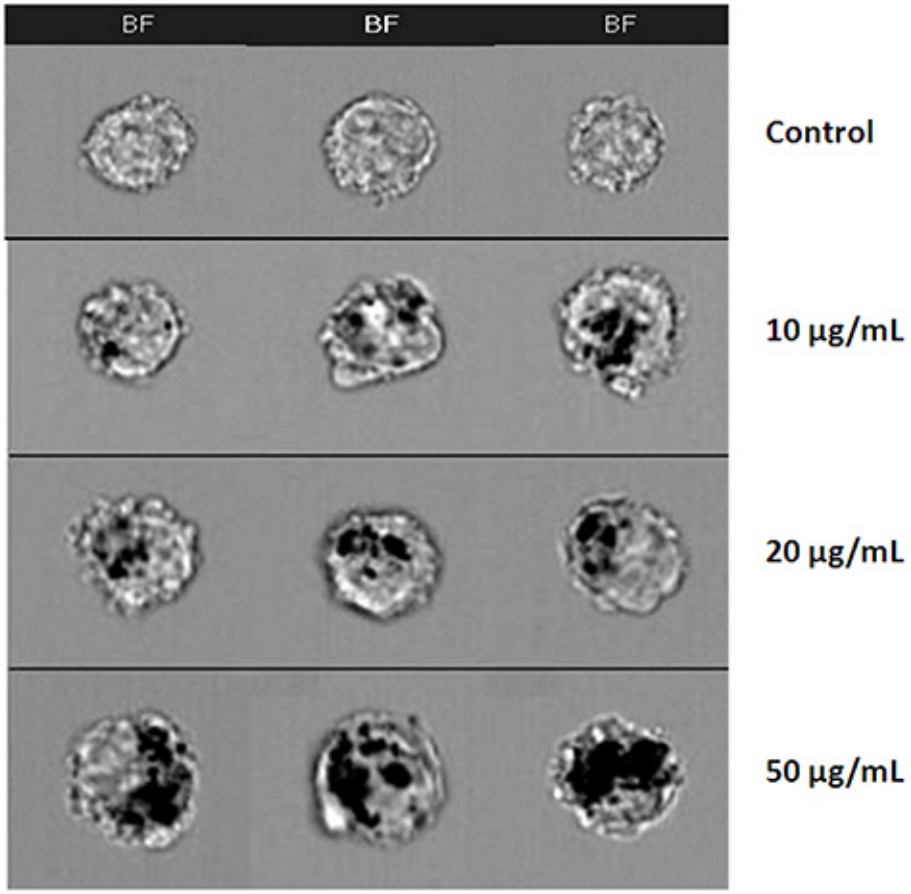

Figure 4. Dose-dependent uptake of CNTs visualized by ImageStream. The number and area of black spots on the bright field images are increasing with the dose of CNTs during incubation with cells (ranging from 0-50 µg/ml). Note that the control cells are devoid of black spots.

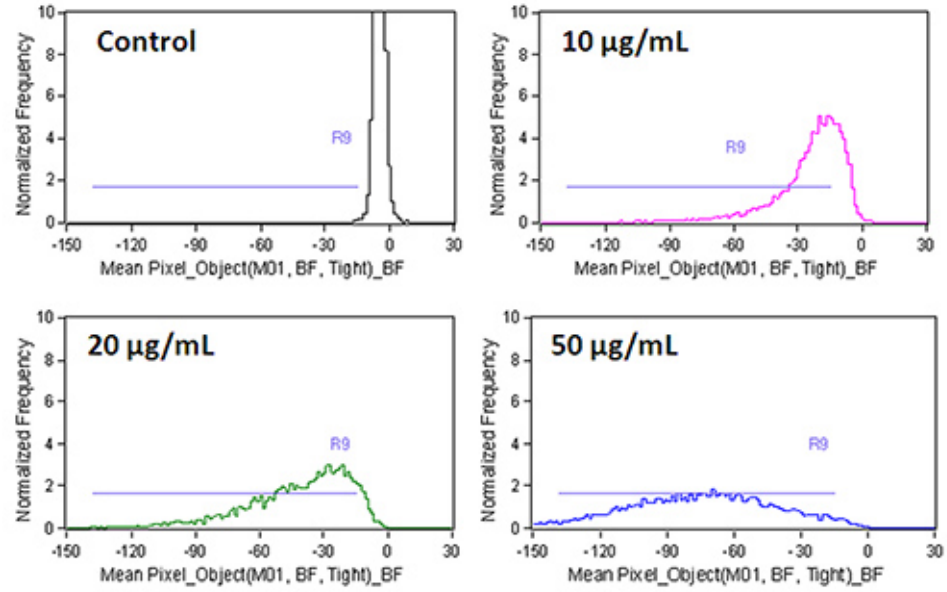

Figure 5. Relative quantification of CNT-uptake based on the bright field images. Histograms of the mean pixel feature applied to the mask "object" featuring the whole cell clearly show a dose-dependent behavior, which can be used for quantification. R9 range encloses the CNT-positive cells.

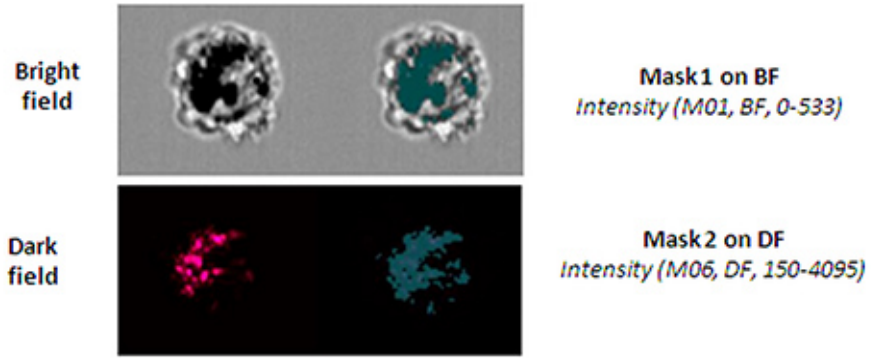

Figure 6. Creation of masks selecting black spots on BF and bright spots on DF images. As CNTs appear as strongly absorbing dark spots on BF image, a threshold mask is created to select a restricted range of pixels with a low intensity comprised between 0-533 in this study *(Mask 1, notation: Intensity(M01, BF, 0-533))*. Conversely, a mask fitting with the pixels of high intensity (150-4095 in this case) on DF image *(Mask 2, notation: Intensity (M06, DF, 150-4095))* is used to select bright spot on DF, corresponding to high scattering areas.

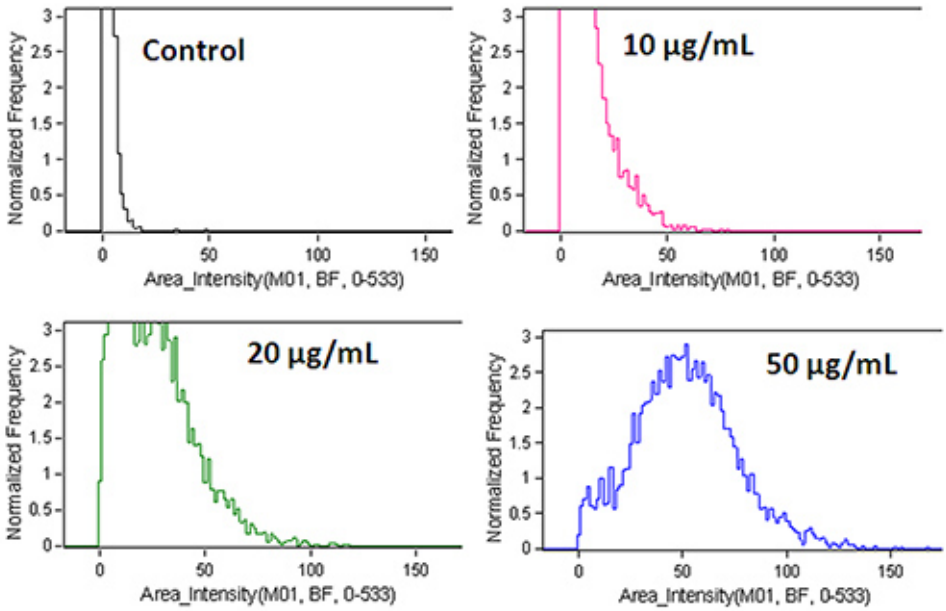

Figure 7. Dose-dependent uptake of CNTs is demonstrated by quantification of the black spot area on BF images. Using threshold mask (*mask 1*) applied on BF, the area of black spots can be quantified for each cell, showing a dose-dependent distribution.

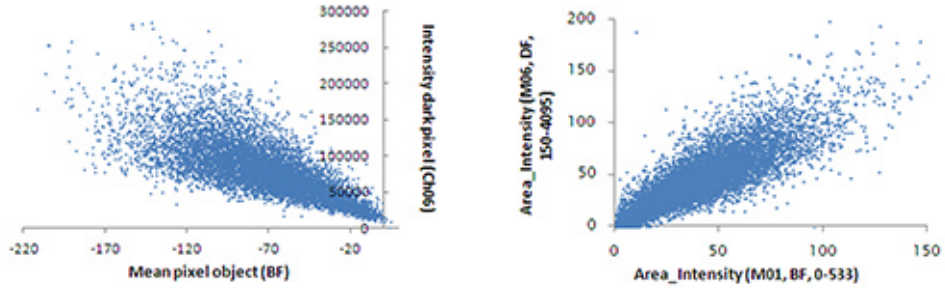

Figure 8. CNT quantification methods based on BF (absorption) and DF (scattering) images are correlated. On the left, mean pixel on the BF image *versus* intensity on the DF image, show a good correlation for cells labeled with CNTs (50 µg/ml) (Pearson correlation coefficient r = -0.68). On the right, area of the mask fitting dark spots on BF *versus* area of the mask fitting bright spots on DF for cells labeled with CNTs (50 µg/ml). Pearson correlation coefficient is r = -0.83.Values from 7,000 cells are plotted.

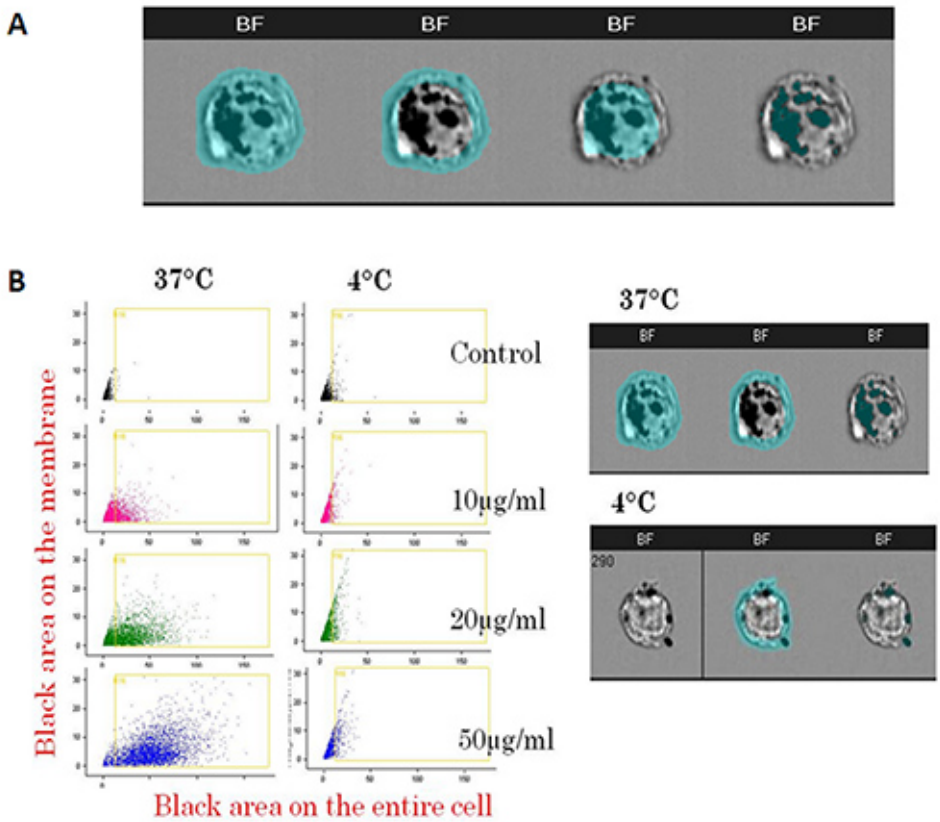

Figure 9. CNT localization in cells using specific masks. (**A**) Masks are created to fit a particular location of the cell, namely from left to right - the entire cell, the membrane only, and the inside of the cell. Another mask fits black spots thanks to a threshold intensity (*Mask 1, notation: Intensity(M01, BF, 0-533)*). (**B**) Assessment of the localization of CNTs can be obtained by measuring the area of black spots on different localizations of the cells using the localization masks described in A. Incubation with CNTs (50 µg/ml) was performed both at 37 °C and at 4 °C to inhibit internalization pathway. The graph representing black area on the membrane versus black area on the entire cell shows a dose-dependent absorption of CNTs on the membrane at 4 °C, while the full internalization of CNTs is effective at 37 °C.

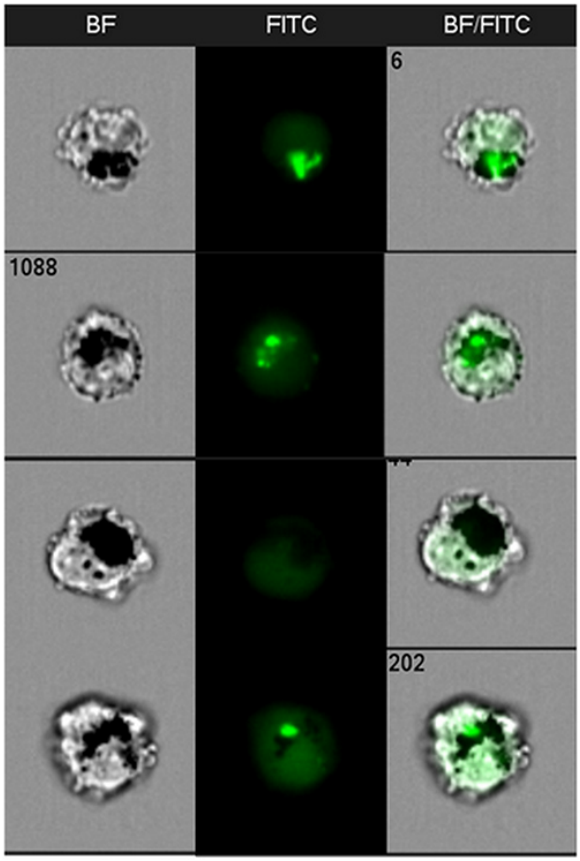

Figure 10. Colocalization of CNT-induced black spots on BF with fluorescence bright spots on FITC image. The fluorescence bright spots are not always colocalized with the black spots on BF. They match properly for the first two cells displayed, but not for the last two cells.

Discussion

1. Modification and Troubleshooting

In this study, the first objective was to evaluate the quantity and the localization of CNTs in cells. The confocal microscopy could have been *a priori* the gold method to assess the intracellular distribution of CNTs functionalized with the fluorescent marker FITC[8,14]. However, the main drawback is the limitation to single cell imaging and, therefore, a lack of statistically relevant data. The ImageStream allows work beyond these obstacles: indeed, by screening a large number of cells (5,000-10,000) in a short time (<min), it yields statistically robust results, enhanced also by the high resolution imaging which provides images for each cell with a subcellular resolution (0.5 µm). It makes then possible to analyze a large amount of data based on single image analysis.

In comparison to conventional flow cytometry, the unique advantage of ImageStream is to provide multispectral *images* of each cell and a pixel by pixel comparison of signal intensity. Thus ImageStream combines the statistical power of high throughput flow cytometry with the analytical advantages of confocal imaging for each analyzed cell. It is crucial for a label-free relative quantification and localization of CNTs in cells.

2. Critical Steps Within the Protocol

The critical step consists of the choice of parameters most suitable of each study. In our case, the best way was to base the analysis on the absorption and scattering properties of the nanotubes: the good correlation between the localization of dark spots on BF and bright spots on DF supports that the developed method is relevant and reliable - and may not have been possible without cell imaging.

3. Limitations of the Technique

It must be emphasized that the visualization of CNTs in cells was possible only because they tend to accumulate in endosomal intracellular vesicles, and then appear as strong absorptive and scattering spots. Individual nanotubes should not be detected based on this method whereas it could be eventually detected on fluorescence, which constitutes a clear limitation. Second, the quantification is not 'absolute' but relative for different labeling concentrations and in comparison to the control unlabeled cells. Some quantitative features (mean pixel, intensity, *etc.*) are absolute parameters, whereas others depend on the choice of the masks (threshold mask, localization masks).

4. Significance with Respect to Existing Methods

In regards to fluorescence, the ImageStream analysis highlights the poor colocalization of CNT clusters between FITC bright signal and spots on the others channels. Therefore, it appears that fluorescence was not a reliable indicator for the quantification and localization of CNTs. Nevertheless, overcoming the limitation of conventional flow cytometry, which is mainly based on fluorescence quantification, the multispectral high throughput ImageStream paves the way for a statistical *label-free* quantification, while providing localization of carbon nanotubes inside the cells.

5. Future Applications

This high throughput statistical nanometrology method could be generalized to any nanomaterials, which show high absorption and scattering of light when interacting with cells. Therefore, it may have important applications for investigations of the nano-bio-interface, nanotoxicology, and nanomedicine.

Disclosures

The authors declare that they have no competing financial interests.

Acknowledgements

This work was supported by ANR P2N (Nanother project 2010-NANO-008-04), by the Region Ile de France (contract no E539), and by CNRS. Open Access was paid for by EMD Millipore.

References

1. Kostarelos, K., Bianco, A. & Prato, M. Promises, facts and challenges for carbon nanotubes in imaging and therapeutics. *Nat. Nano.* **4**, 627-633 (2009).
2. De La Zerda, A. *et al.* Carbon nanotubes as photoacoustic molecular imaging agents in living mice. *Nat. Nano.* **3**, 557-562 (2008).
3. Zavaleta, C. *et al.* Noninvasive Raman Spectroscopy in Living Mice for Evaluation of Tumor Targeting with Carbon Nanotubes. *Nano Lett.* **8**, 2800-2805 (2008).
4. Tong, L. *et al.* Label-free imaging of semiconducting and metallic carbon nanotubes in cells and mice using transient absorption microscopy. *Nat. Nano.* **7**, 56-61 (2012).
5. Welsher, K. *et al.* A route to brightly fluorescent carbon nanotubes for near-infrared imaging in mice. *Nat. Nano.* **4**, 773-780 (2009).
6. Jin, H., Heller, D. A., Sharma, R. & Strano, M. S. Size dependent cellular uptake and expusion of single-wall carbon nanotubes: single particle tracking and a generic uptake model for nanoparticles. *ACS Nano.* **3**, 149-158 (2009).
7. Al-Jamal, K. T. *et al.* Cellular uptake mechanisms of functionalised multi-walled carbon nanotubes by 3D electron tomography imaging. *Nanoscale.* **3**, 2627-2635 (2011).
8. Reuel, N. F., Dupont, A., Thouvenin, O., Lamb, D. C. & Strano, M. S. Three-Dimensional Tracking of Carbon Nanotubes within Living Cells. *ACS Nano.* **6**, 5420-5428 (2012).
9. Phanse, Y., Ramer-Tait, A. E., Friend, S. L., Carrillo-Conde, B., Lueth, P., Oster, C. J., et al. Analyzing Cellular Internalization of Nanoparticles and Bacteria by Multi-spectral Imaging Flow Cytometry. *J. Vis. Exp.* (64), e3884, doi:10.3791/3884 (2012).
10. Qian, F., Montgomery, R. R. Quantitative Imaging of Lineage-specific Toll-like Receptor-mediated Signaling in Monocytes and Dendritic Cells from Small Samples of Human Blood. *J. Vis. Exp.* (62), e3741, doi:10.3791/3741 (2012).
11. Marangon, I. *et al.* Intercellular Carbon Nanotube Translocation Assessed by Flow Cytometry Imaging. *Nano Lett.* **12**, 4830-4837 (2012).
12. Lacerda, L. *et al.* Translocation mechanisms of chemically functionalised carbon nanotubes across plasma membranes. *Biomaterials.* **33**, 3334-3343 (2012).
13. Al-Jamal, K. T. & Kostarelos, K. *Methods in Molecular Biology.* Kannan Balasubramanian, Marko Burghard. ed. Humana Press, Vol. 625, 123-124 (2010).
14. Zhou, F. *et al.* New Insights of Transmembranal Mechanism and Subcellular Localization of Noncovalently Modified Single-Walled Carbon Nanotubes. *Nano Lett.* **10**, 1677-1681 (2010).